Effects of Image Processing on Electron Diffraction Patterns Used for Nanobeam Diffraction Strain Measurements

Mark J. Williamson[1], Piet van Dooren[1], and John Flanagan[2]
[1]FEI Company Eindhoven Netherlands & [2]Hillsboro, Oregon

Introduction

For more than 60 years it has been known that mechanical strain can increase carrier mobility in semiconductor materials, [1]. More recently strained silicon has been introduced into the manufacturing of electronic and optical devices. Strain engineering has helped semiconductor manufacturers keep up with Moore's scaling [2]. Moving forward the International Technology Roadmap for Semiconductors suggests that both technological and manufacturing benefits could come from the use of strained germanium or III-V materials [3]. Motivated by the need of strain engineering, strain measurement at the nanometer level is a topic of major interest in the semiconductor industry.

Typically strain in nanometer scale devices is measured with the transmission electron microscope (TEM). Several techniques are available for strain measurements in the TEM including but not limited to, nanobeam electron diffraction (NBD) [5,6], dark-field electron holography (DFEH) [7-9], convergent beam electron diffraction (CBED) [10], and HRTEM geometric phase analysis (GPA) [11]. Of these techniques nanobeam electron diffraction produces the most direct path to data analysis and is generally considered the easiest and most productive technique for reliable strain measurement.

Nanobeam Electron Diffraction (NBD)

The positions of the reflections in an electron diffraction pattern (DP) are inversely proportional to the spacing of the lattice planes which produce the reflection. Therefore, by measuring the shifts in diffraction pattern reflections it is possible to measure the changes in the spacing of lattice planes or strain. With typical conditions, sub-pixel ($<1/10^{th}$ pixel) measurement precision of the reflection positions is required for strain measurement in electronic materials.
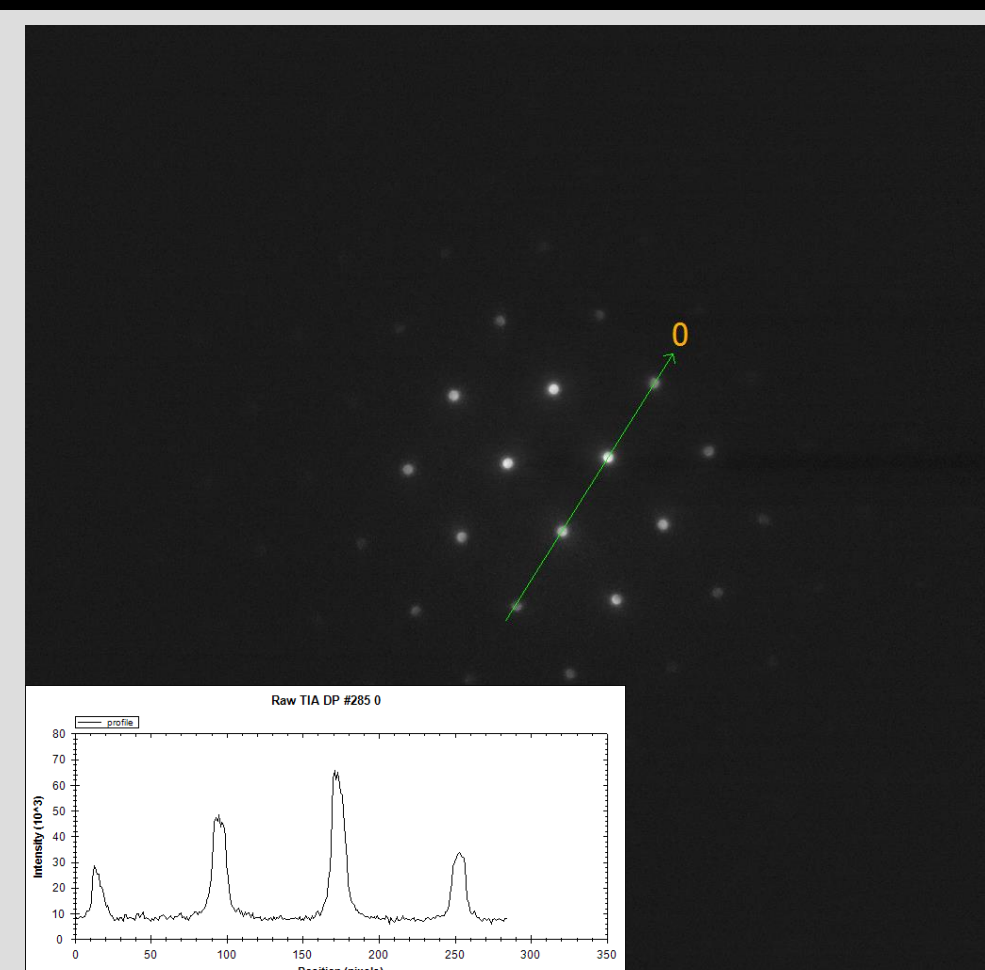
Figure 1: Example [110] electron diffraction pattern from a silicon sample. The half convergence angle is 0.2 mrad and the electron probe is approximately 4nm.

For the past 8 years the FEI Company has offered a package, True Crystal, for recording and analyzing NBD data. Over the last 18 months FEI has been testing and coding a new software package (Epsilon) to replace the software component of True Crystal. In doing this engineers have reviewed the algorithms and image processing techniques used for NBD measurements. In particular significant effort has been invested in reviewing the peak fitting algorithms and image processing associated with this analysis. The algorithms used to process nanobeam electron diffraction patterns become more important as the required spatial resolution of the technique decreases below approximately 4 nanometers.

A three condenser Titan microscope can make a parallel electron probe to approximately 5 nm. Making a smaller probe requires converging the beam. Figure 1 shows a diffraction pattern recorded with half convergence angle of 0.2 mrad creating an approximately 4 nm electron probe. The inset shows the intensity profile defined by the thin green line drawn on the image. The reflections are relatively uniform. Figure 2

shows an electron diffraction pattern recorded with a half convergence angle of 0.71mrad and a 1-2 nm probe. In this image the reflections and the profile show significant non-uniformity and asymmetry..

Two processes contribute to the variation in the reflection of image First, dynamical diffraction causes the intensity variation seen in the individual reflections. The second effect is the increase in the size of the diffraction reflections which is a result of a finite convergence angle of the beam. These two processes make determining the centers with sub pixel accuracy more difficult than simple peak fitting.
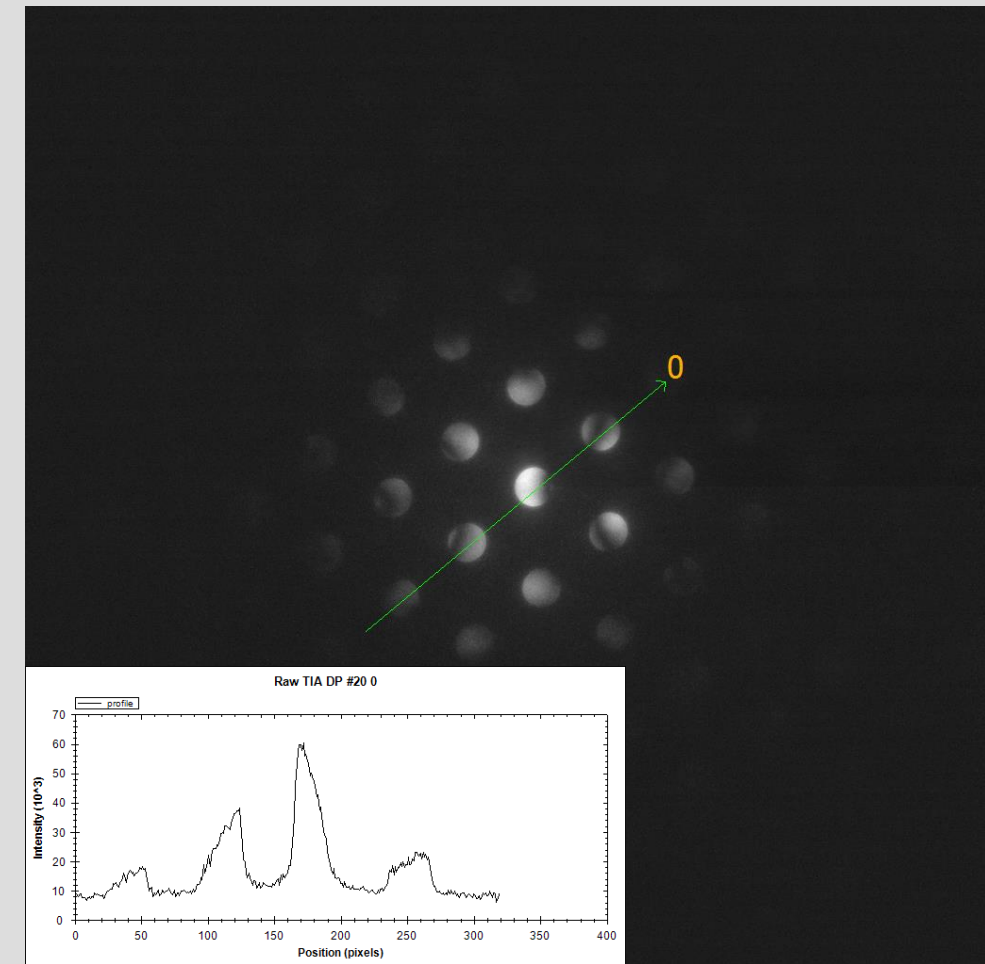
Figure 2: Example [110] electron diffraction pattern from a silicon sample. The convergence angle is 0.71 mrad and the electron probe is approximately 1-2 nm.

Strain Algorithm

Nanobeam electron diffraction is a relative technique in that strain is measured with respect to a diffraction pattern of known strain (typically 0). The algorithm for computing strain from electron diffraction data involves determining the positions of the reflections in the diffraction pattern very accurately. Typically the diffraction patterns are filtered in some method to strengthen the signal in the image. After this filtering the reflections in the DP are grossly determined based on known basis vectors. Then the reflections are fit using a more accurate method including linear least squares fitting to a surface or various methods of fitting cross-sections of the reflections. The peak positions are then used to determine the best two vectors capable of reproducing the entire diffraction pattern. These two new vectors are then used to recreate the diffraction pattern for the strain calculation. The strain is calculated by comparing the refined reflections in reference diffraction patterns and the diffraction patterns to be measured.

Image processing

Each of 4 reflection fitting routines were constructed and tested using 5 data sets. Two of the fitters had two variants and all were tested with and without performing an autocorrelation prior to fitting. Two additional fitters were tested from the previous software generation. This resulted in 14 variants. Each routine begins by isolating the individual reflections based on a percentage of the diffraction vector length. The routines were:

- Paraboliod fitter: This method fits a paraboloid to each reflection in the diffraction pattern.

- Circle fitter: This fitter thresholds each reflection and fits a circle to the resulting binary image. This fitter was tested in two variants. In the first variant the threshold value was defined as a user input as a percentage of the total peak height. In the second variant, the peaks threshold values were dynamically determined based on changes in the slope of the reflection.

- Ellipse fitter: Same as the circle but fit an ellipse rather than a circle.

- Disk fitter: Similar to the circle and ellipse fitters however the fit is performed by fitting a circle to the reflection convex hull using a Nelder-Mead simplex minimizer.
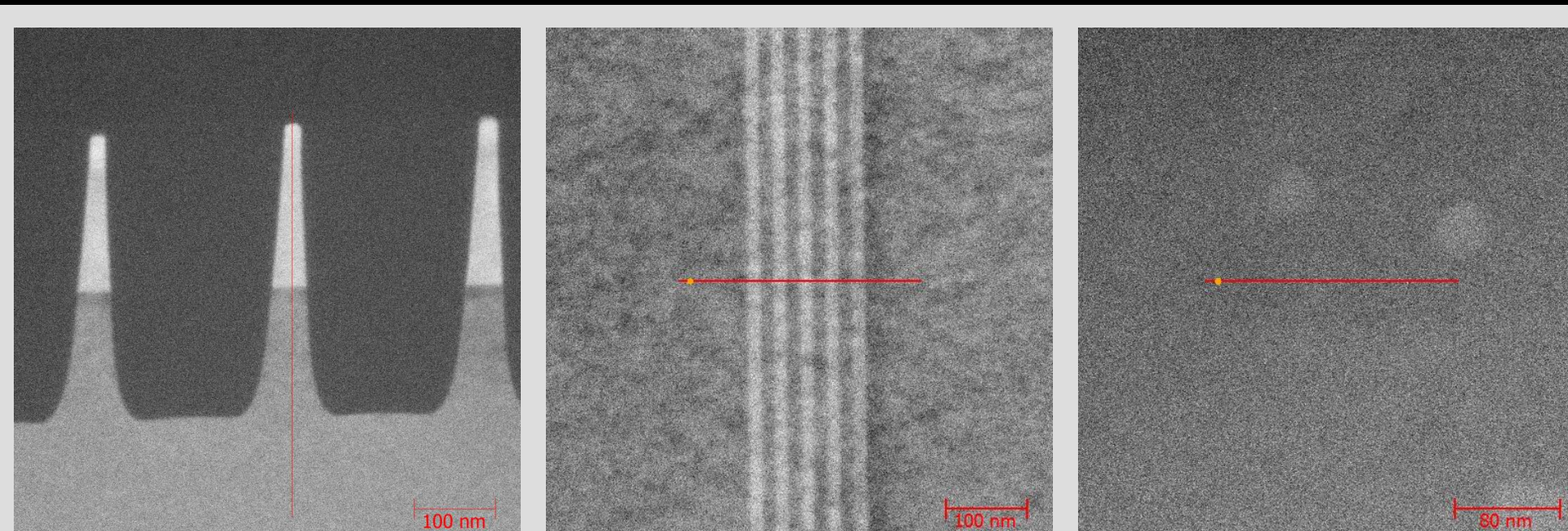
Test Samples

Figure 3: Three of the five samples used to test the NBD algorithms. On the left are Si/SiGe/Ge pillars, in the center is a Mag*i*cal sample with 5 SiGe lines and on the right is bare silicon.

Five samples were used to test the NBD algorithms. These include 4 types of SiGe structures or blanket films and one sample of bare silicon. Three of the samples are shown in figure 3. The SiGe samples were chosen because the Si/Ge or Ge lattice can be used as a proxy for strain. Each of the 5 data sets were run with using each of the 14 variants of the strain algorithms.

Regions of uniform strain within each sample were used to test the sensitivity of the algorithms and the effect of the autocorrelation. These sensitivities were determined using the standard deviations of the strain in the [002] and [220] directions, (one sample did not have a strain free region in the [002] direction and was excluded from the analysis). Figure 4 shows the strain profiles in the two [002] and [220] directions for the samples shown in figure 3.
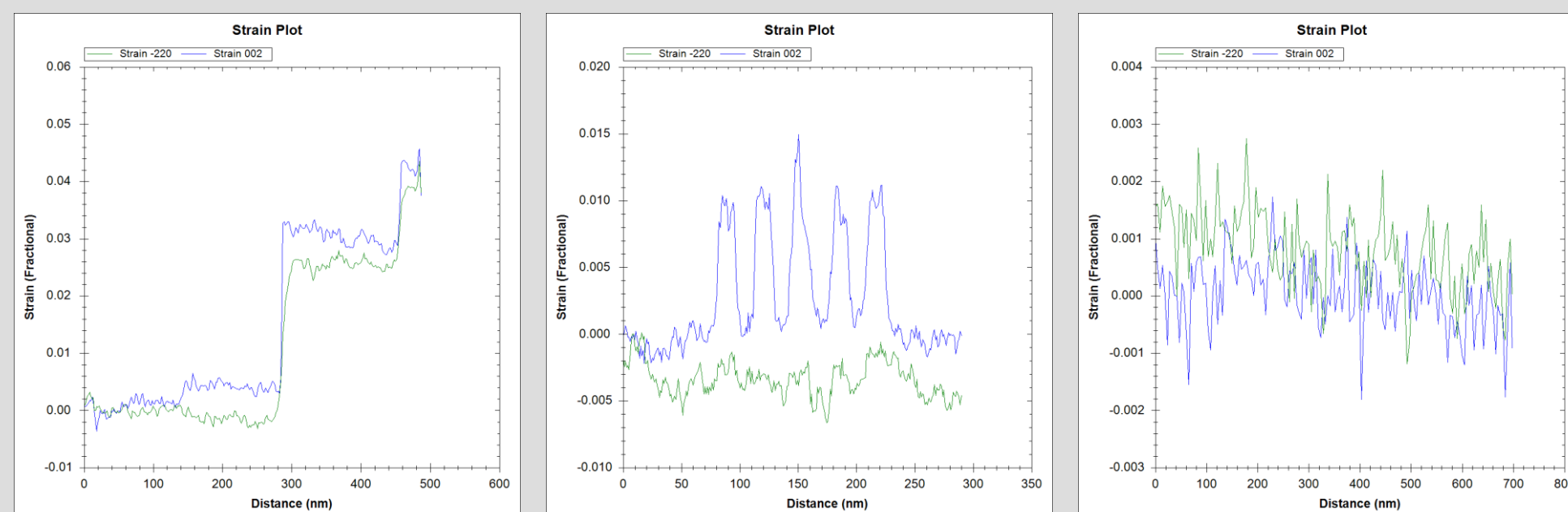

Figure 4 shows the strain profiles for the three samples shown in figure 3.

Analysis

The experiment was designed and statistically analyzed with the Design Of Experiment (DOE) methodology. This method is used to systematically investigate process variable that influence product quality. In this case the measure of product quality was the standard deviation of the strain in 002 and 220 directions. The results shown herein focus on determining the best reflection finding algorithm and the effect of the autocorrelation. Figure 5 shows the main effects plots for these results using the sensitivities of the [002] and [220] directions. The probability values for the tests related to determining the best peak fitting algorithm were 0.85 and 0.48 respectively for the data in the [002] and [220] directions. These values are well above 0.05 and are not statistically significant. Therefore, it was not possible to determine the best peak fitting algorithm with statistical significance. This result is further confirmed by the box plots shown in figure 6. The fact that the box plots all overlap one and other demonstrated a lack of uniqueness and suggests that none are either much better or worse than the rest for the 5 datasets investigated. All data new algorithms performed better than the existing TC algorithm.

The right side plots in figure 5 show a strong and almost identical effect of the autocorrelation on the data analyzed. This data shows that using the autocorrelation strongly influences the sensitivity of the data processed. The p value for this effect was 0.003 in both directions. Autocorrelation has a strong and statistical significant positive effect (p-value must be < 0.05 to be significant).
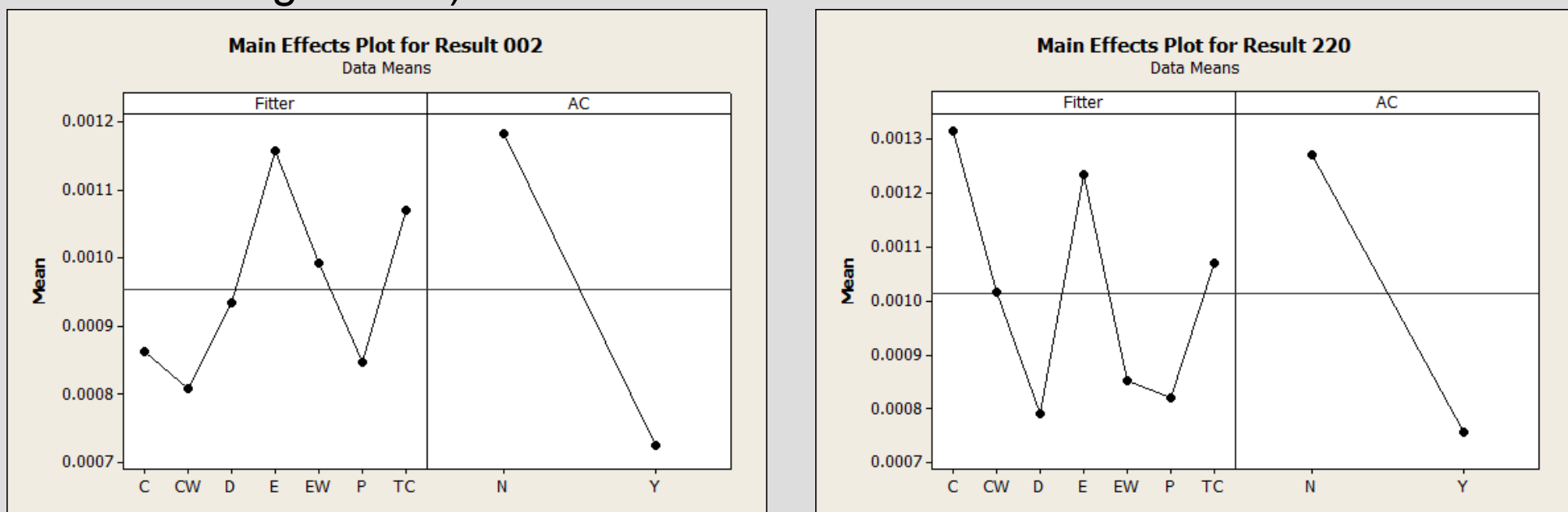

Figure 5: The main effects plots used to determine the best peak fitting routine and the effect of the autocorrelation.
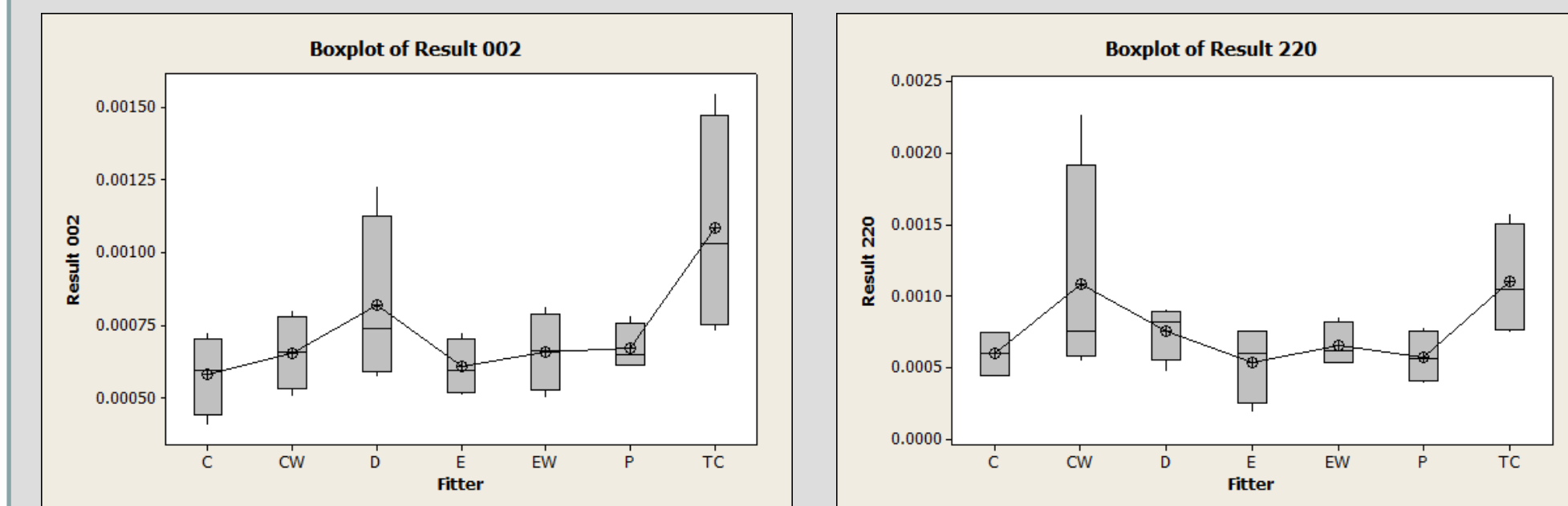
Analysis Continued

Figure 6: Box plots showing the correlation of the various fitters.

AutoCorrelation

In order to better understand the effect of the autocorrelation a simple 2D periodic structure with a linear envelope was simulated by adding Gaussian peaks at 64 pixel intervals to a 1024 pixel length signal. Noise was added to the peaks at levels of 0.7, 1.5 and 3.0 percent of the maximum peak height before autocorrelation. The peaks were then re-fit and the new centers were determined. 10,000 simulation runs were executed and the average peak positions were determined. These average peak positions are equivalent to a diffraction vector in NBD analysis. Figure 7 shows the mean and standard deviations of these measurements as a function of reflections used in the averaging. Two things are apparent from the data. First, the variation in the measurements decreases with the number of reflections (peaks) used in the analysis. Second, the autocorrelation results in deviations from the known peak spacing.
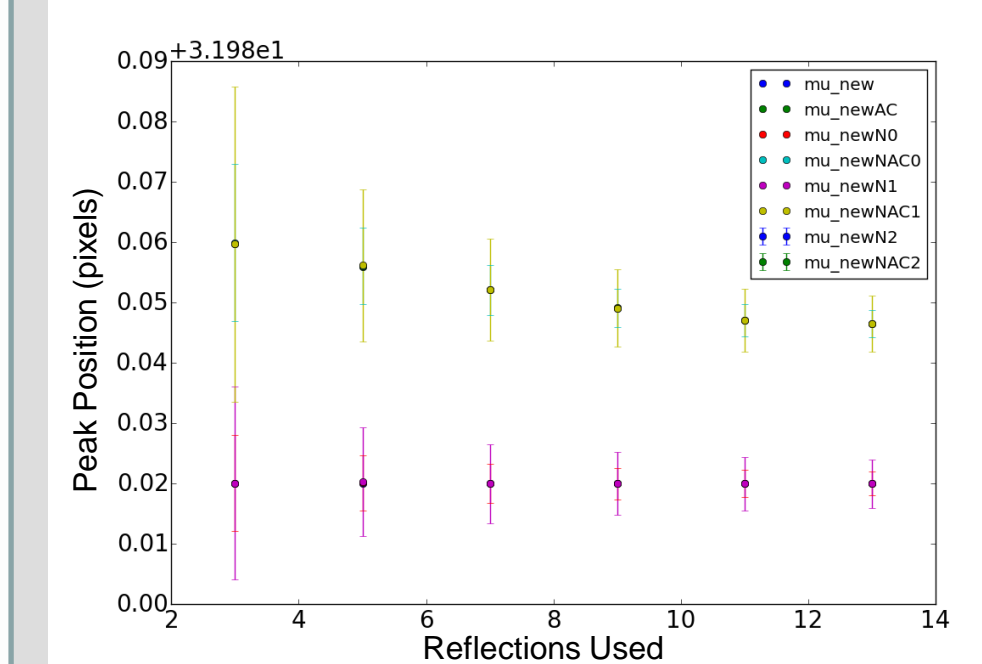

The deviations in the peak positions do not pose a problem for NBD analysis because it is a relative technique so as long as the offsets are constant it will not effect the accuracy of the technique. While the decrease in the sensitivity with increasing number of reflections is a likely reason the experimental data is always better with the autocorrelation. Table 1 shows the number of peaks used in determining the strain for the experimental data shown in this paper. Using the autocorrelation results in using an average of 60% more peaks in the analysis. Further analysis is required to determine how the autocorrelation effects diffraction data with dynamical contrast in the reflections.

Figure 7: Mean and standard deviation of simulations.

Filter	AC	D01	Lower	NBD02	SIMS	V1
CW	Y	73	78	67	80	70
CW	N	11	20	14	49	30
C	Y	73	74	73	79	70
C	N	21	20	15	57	30
D	Y	53	72	65	67	71
D	N	18	25	9	57	36
EW	Y	73	78	75	80	72
EW	N	11	19	12	49	35
E	Y	73	74	73	79	64
E	N	20	19	10	57	31
P	Y	73	81	74	81	34
P	N	30	29	15	71	45
TC	Y	0	0	0	0	0
TC	N	0	0	0	0	0

Table 1: Peaks used in experimental fits.

Conclusions

Nanobeam electron diffraction data was analyzed to determine the best peak fitting routine for a combination of 5 data sets. This was done using a combination of 7 peak fitting routines with and without the autocorrelation. Although it was not possible to determine a global best fitting routine for all of the data, the effect of the autocorrelation was statistically significant in producing more data with a smaller standard deviation of the strain data in regions of known constant strain.

Future Work

Future work will focus on both better understanding the effect of the autocorrelation on the processing of diffraction data and on determining the best conditions for acquiring NBD data. The fitting routines will be analyzed both with respect to the accuracy and the sensitivity of the technique. This will be done by using the fitting routines described above to process diffraction data from idealized simulation, more realistic dynamical simulations, and simplified NBD data recorded under various conditions. This later data will also be used to optimize the conditions for data acquisition.

References

1. C.S. Smith, *Phys. Rev.* **9**, 42-49, (1954).
2. S.E. Thompson et. Al., *IEEE Transactions on Electron Devices*, **51**(11), 1790-1797, (2004).
3. S.E. Thompson et. Al., *IEEE Transactions on Electron Devices*, **56**(5), 1010-1020, (2006).
4. www.ITRS.net
5. A. Beche et al. Applied Physics Letters, **95** 123114 (2009).
6. P. Favia et al. Journal of the Electrochemical Society, **158**(4) H438-H446 (2011).
7. F. Hue et al. Applied Physics Letters, **95**, 073103, (2009).
8. Cooper et Al. Applied Physics Letters, **96**, 113508, (2010).
9. Y.Y. Wang et. Al. Ultramicroscopy, 124, 117-129 (2013).
10. Applied Physics Letters, 86. 063508, (2005).
11. M.J. Hytch, Ultramicroscopy 74, 131-146 (1998).

Contact Information

Mark.Williamson@fei.com

www.fei.com
5350 NE Dawson Creek Drive
Hillsboro, OR 97124
Phone: +1 (503).726.7500